East European Journal of Physics. 1. 473-483 (2026)
DOI:10.26565/2312-4334-2026-1-54 ISSN 2312-4334

FDM SIMULATION OF Cu–Al_2O_3/WATER CASSON HYBRID NANOFLUID FLOW AND THERMAL TRANSPORT IN A COUETTE SYSTEM

Khasim Ali[1], Ramesh Alluguvelli[2], Swatmaram[3], Chandra Shekar Balla[4]*, K. Praveen Kumar[5], E. Jagathprabhav[6]

[1]*Department of Mathematics, Nawab Shah Alam Khan College of Engineering and Technology, Hyderabad, Telangana, 500024, India*
[2]*Department of Mathematics, Geethanjali College of Engineering and Technology, Keesara, Hyderabad, Telangana, 501303, India*
[3]*Department of Mathematics, Chaitanya Bharathi Institute of Technology, Hyderabad, Telangana, 500075, India*
[4]*Government Junior College, Amangal, Ranga Reddy, Telangana, 509321, India*
[5]*Department of Humanities and Science, Government Polytechnic, Hyderabad, Telangana, 500028, India*
[6]*Department of Humanities and Science, Government Polytechnic, Shadnagar, Telangana, 509216, India*
**Corresponding author's email: shekar.balla@gmail.com*
Received December 2, 2025; revised January 19, 2026; accepted January 27, 2026

This paper numerically inspects the unsteady Couette Casson hybrid nanofluid (HNF) containing copper (Cu) and aluminum oxide (Al_2O_3) nanoparticles dissolved in water. The upper wall is set in uniform motion, and the lower wall is taken as stationary and stretchable. Finite difference method (FDM) is used to integrate the governed nonlinear partial differential equations. The results are explored through streamlines, isotherms, Nusselt number and skin friction. The impact of key dimensionless numbers such as Grashof number, Biot number, stretching parameter, Casson parameter, and Eckert number on Cu-Al_2O_3-water HNF is discussed. The results disclose that the flow and heat transfer(HT) can be controlled considerably by the key parameters.
Keywords: *Couette flow; Variable viscosity; Al_2O_3-H_2O nanofluid; Biot number; Stretching parameter*
PACS: 47.11.-j, 47.50.-d, 47.61.-k, 44.25.+f

1. INTRODUCTION

In recent years, substantial attention has been garnered by non-Newtonian fluid flows because of their extensive applications in engineering, biomedical, and industrial processes. Casson fluid model is one to describe non-Newtonian behaviour and captures effectively the yield-stress characteristics of materials like paints, polymer solutions, blood, and printing inks. This model was first introduced by Casson [1] in 1959. Mukhopadhyay[2] analysed HT in Casson flow over a stretchable surface. Abd El-Aziz and Afify [3] inspected MHD Casson flow with entropy generation. Previous investigations [4-8] have addressed Casson fluid flow over stretching surfaces, porous media, and boundary layers under the influence of magnetic fields, thermal radiation, viscous dissipation, and entropy generation. Several authors [9-13] confirmed Casson rheology's role in predicting realistic non-Newtonian flow behaviour in different configurations. These studies demonstrate the effectiveness of the Casson model in capturing realistic non-Newtonian behaviour, however, most are restricted to steady or external boundary-layer flows.

In parallel, nanofluid technology introduced to enhance thermal transport properties by dispersing nanoparticles into base fluids, has become a significant development in modern HT enhancement[14]. Tiwari and Das [15] studied the nanofluid flow in square cavity. Mono-nanofluids have been widely explored for various geometries and thermal conditions [16–20]. More recently, HNFs are made by combining two or more types of nanoparticles. Due to the synergistic effects between different particle materials, they exhibit improved thermal performance. Such hybrid suspensions exhibit superior HT capability, stability, and regulable viscosity. Unlike mono-nanoparticle nanofluids, HNFs highly associated to cooling systems, energy systems, and process engineering. Studies on Al_2O_3–Cu/water and related hybrid nanofluids with radiation and porous effects have reported notable enhancements in thermal efficiency [21–25].

Couette flow, representing the motion of a viscous fluid lying in two parallel plates with one or both plates in relative motion, serves as a fundamental configuration for studying shear-driven transport phenomena. Attia et al. [26] studied how temperature dependent viscosity and thermal conductivity influence unsteady hydromagnetic Couette flow. Couette flow is further studied by several researchers [27-33]. Existing studies have largely focused on steady-state flows or single-nanoparticle suspensions. In many practical applications, including lubrication systems and transient electronic cooling, the flow and temperature fields are naturally unsteady. Therefore, unsteadiness is incorporated to capture the transient evolution of the system. These transient effects are particularly important for accurately describing the behaviour of non-Newtonian hybrid nanofluids. Zeeshan et al. [34] studied MHD Casson hybrid nanofluid over the shrinking sheet. Although recent works have investigated Casson hybrid nanofluids in various geometries [35–42], the combined effects of unsteadiness, Casson and hybrid nanoparticle dispersion within an internal Couette geometry remain insufficiently explored.

Recent research [43-47] has focused on Casson hybrid nanofluids, where two or more distinct nanoparticles are dispersed in a Casson base fluid to achieve superior thermophysical performance. However, most prior studies have been

Cite as: K. Ali, R. Alluguvelli, Swatmaram, C.S. Balla, K.P. Kumar, E. Jagathprabhav, East Eur. J. Phys. 1, 473 (2026), https://doi.org/10.26565/2312-4334-2026-1-54

limited to steady, external boundary-layer configurations such as stretching sheets or porous media, neglecting unsteady internal geometries like Couette channels. The effects of unsteadiness and HT for Casson HNF in a Couette configuration are still not well understood. Therefore, present study aims to address this gap by investigating unsteady Casson HNF flow and HT between parallel plates. This analysis contributes new insights into non-Newtonian hybrid thermal transport under confined geometries.

Motivated by this gap, the current work examines the unsteady Couette flow of a Casson HNF consisting of Copper (Cu) and alumina (Al_2O_3) nanoparticles dispersed in water. The upper wall of the channel is moving uniformly, while the lower wall is stationary and stretchable. A comprehensive mathematical formulation incorporating the impact of key dimensionless parameters such as the Casson parameter, Grashof number, Biot number, stretching parameter, and Eckert number is developed. The governing nonlinear partial differential equations are solved using a finite difference method (FDM) to elucidate the fluid flow and HT characteristics.

2. MATHEMATICAL FORMULATION

An unsteady, laminar, incompressible Casson HNF flow of Cu-Al_2O_3-H_2O confined within two parallel plates is taken into account. The viscosity of the fluid is considered to be a function of temperature. To configure the model geometry, x-axis is aligned with the plate and the y-axis is oriented perpendicular to the plates, as shown in Figure 1. The lower plate is located at y =0, possesses a stretching velocity U_0. The upper plate had convective cooling at y = h. And this flow is driven by a uniform pressure gradient located at the ends of the channel.

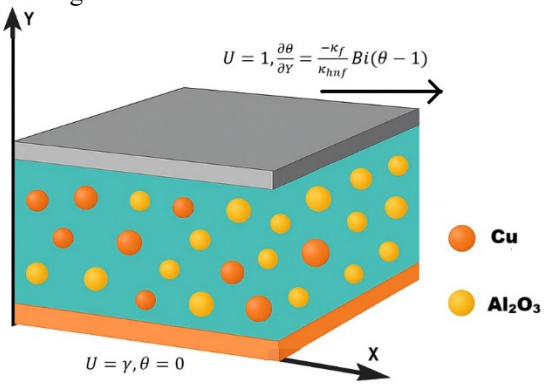

Figure 1. Physical configuration

Based on Tiwari and Das [15] nanofluid model for nanofluid, the governing equations are given by,
Momentum equation:

$$\rho_{hnf}\frac{\partial u}{\partial \tau} = -\frac{\partial p}{\partial x} + \left(1 + \frac{1}{\lambda}\right)\frac{\partial}{\partial y}\left(\mu_{hnf}(T)\frac{\partial u}{\partial y}\right) + (\rho\beta_T)_{hnf} g(T - T_0) \tag{1}$$

Temperature equation:

$$\frac{\partial T}{\partial \tau} = \alpha_{hnf}\frac{\partial^2 T}{\partial y^2} + \frac{\mu_{hnf}(T)\,\alpha_{hnf}}{\kappa_{hnf}}\left(\frac{\partial u}{\partial y}\right)^2 \tag{2}$$

The dynamic viscosity is presumed to be an exponential declining function that depends on temperature [28], expressed as,

$$\mu_f(T) = \mu_0 e^{-m(T - T_0)} \tag{3}$$

Constraints at the boundary are:

When $\tau = 0$, $\quad u = 0, T = 0 \quad$ at $\quad y = 0,\ y = h$

$$\text{When } \tau > 0, \quad \left.\begin{array}{ll} u = U_0, \ T = T_0 & \text{at} \quad y = 0 \\ u = U_h, -\kappa_{hnf}\dfrac{\partial T}{\partial y} = h_f(T - T_\infty) & \text{at} \quad y = h \end{array}\right\} \tag{4}$$

where U_0 corresponds to stretching velocity of bottom plate, U_h denotes velocity of top plate, T_∞ depicts the ambient temperature, P represents nanofluid pressure. μ_0 symbolizes dynamic viscosity of nanofluid at reference temperature T_0 and m represents parameter of viscosity, h_f symbolizes coefficient of HT. Volume fraction of comprised nanoparticles, density, thermal conductivity, thermal diffusivity and heat capacitance are described below. The subscripts f, s, nf and hnf refer to base fluid, solid nanoparticles, nanofluid and hybrid nanofluid. Relationships indicating the physical characteristics of nanofluids are expressed as:

$$\mu_{hnf} = \frac{\mu_f}{(1-\phi_1)^{2.5}(1-\phi_1)^{2.5}} \tag{5}$$

$$\rho_{hnf} = \left\{(1-\phi_2)\left((1-\phi_1)+\phi_1\frac{\rho_{s1}}{\rho_f}\right)+\phi_2\frac{\rho_{s2}}{\rho_f}\right\}\rho_f \tag{6}$$

$$(\rho C_P)_{hnf} = \left\{(1-\phi_2)\left((1-\phi_1)+\phi_1\frac{(\rho C_P)_{s1}}{(\rho C_P)_f}\right)+\phi_2\frac{(\rho C_P)_{s2}}{(\rho C_P)_f}\right\}(\rho C_P)_f \tag{7}$$

$$\kappa_{hnf} = \frac{(\kappa_{s2}+2\kappa_f)-2\phi_2(\kappa_f-\kappa_{s2})}{(\kappa_{s2}+2\kappa_f)+\phi_2(\kappa_f-\kappa_{s2})}\kappa_{nf} \tag{8}$$

$$\kappa_{nf} = \frac{(\kappa_{s1}+2\kappa_f)-2\phi_1(\kappa_f-\kappa_{s1})}{(\kappa_{s1}+2\kappa_f)+\phi_1(\kappa_f-\kappa_{s_1})}\kappa_f \tag{9}$$

$$\alpha_{hnf} = \frac{\kappa_{hnf}}{(\rho C_P)_{hnf}} \tag{10}$$

Table 1. Thermophysical characteristics of Copper, Alumina and Water

Physical characteristics	Cu	Al_2O_3	H_2O
C_p (J/KgK)	385	765	4179
ρ (Kg/m^3)	8933	3970	997.1
k (W/mK)	400	40	0.613

The following dimensionless quantities and parameters are invoked to change governing equations into non-dimensional form.

$$\left.\begin{aligned} X=\frac{x}{h}, Y=\frac{y}{h},\ U=\frac{hu}{\nu_f}, t=\frac{\tau\nu_f}{h^2},\ \theta=\frac{T-T_0}{T_\infty-T_0}, Pr=\frac{\nu_f}{\alpha_f} \\ \bar{P}=\frac{Ph^2}{\rho_f{\nu_f}^2}, \beta=m(T_\infty-T_0),\ Ec=\frac{{\nu_f}^2}{C_P(T_\infty-T_0)h^2}, Bi=\frac{h\,h_f}{\kappa_f}, \gamma=\frac{U_0}{h} \end{aligned}\right\} \tag{11}$$

The converted dimensionless equations could be written as:

$$\frac{\partial U}{\partial t} = \frac{\rho_f}{\rho_{hnf}}\left\{-\frac{\partial\bar{P}}{\partial X}+\left(1+\frac{1}{\lambda}\right)\frac{\mu_{hnf}}{\mu_f}e^{-\beta\theta}\left[\frac{\partial^2 U}{\partial Y^2}-\beta\frac{\partial\theta}{\partial Y}\frac{\partial U}{\partial Y}\right]\right\}+Gr\,\theta \tag{12}$$

Temperature equation:

$$\frac{\partial\theta}{\partial t} = \frac{(\rho C_P)_f}{(\rho C_P)_{hnf}}\left\{\frac{1}{Pr}\frac{\kappa_{hnf}}{\kappa_f}\frac{\partial^2\theta}{\partial Y^2}+\frac{\mu_{hnf}}{\mu_f}e^{-\beta\theta}Ec\left(\frac{\partial U}{\partial Y}\right)^2\right\} \tag{13}$$

Boundary conditions are:

When $t=0$, $\quad U=0,\ \theta=0 \quad$ at $\quad Y=0,\ Y=1$

When $t>0$,
$$\left.\begin{aligned} U=\gamma, \theta=0 \quad & \text{at} \quad Y=0 \\ U=1, \frac{\partial\theta}{\partial Y}=\frac{-\kappa_f}{\kappa_{hnf}}Bi(\theta-1) \quad & \text{at} \quad Y=1 \end{aligned}\right\} \tag{14}$$

Local coefficients of skin friction and Nusselt for lower and upper plates are given by

$$\left.\begin{aligned} C_{f0}=\frac{\mu_{hnf}}{\mu_f}e^{-\beta\theta}\frac{\partial U}{\partial Y}_{Y=0},\ C_{f1}=\frac{\mu_{hnf}}{\mu_f}e^{-\beta\theta}\frac{\partial U}{\partial Y}_{Y=1} \\ Nu_0=-\frac{\kappa_{hnf}}{\kappa_f}\frac{\partial\theta}{\partial Y}_{Y=0}, Nu_1=-\frac{\kappa_{hnf}}{\kappa_f}\frac{\partial\theta}{\partial Y}_{Y=1} \end{aligned}\right\} \tag{15}$$

3. METHODOLOGY

The nonlinear coupled partial differential equations (12-13), with constraints (14), are evaluated numerically using finite difference method. Time derivative is computed with forward difference scheme and spatial derivatives of first and second order with central difference scheme. Convergence of the scheme is assumed when the values of unknowns U, θ of two consecutive iterations differ by less than 10^{-5} i.e., $|\varphi^{n+1}-\varphi^n| \le 10^{-5}$, where n specifies number of loops and φ stands for $[U,\theta]^T$. Table 2 shows the comparison of Cf_{avg} and Nu_{avg} of current study with previous works and found satisfactory.

Equations (12-13) could be written as:

$$\frac{\partial U}{\partial t} = A_1 + A_2\,e^{-\beta\theta}\frac{\partial^2 U}{\partial Y^2} - A_3 e^{-\beta\theta}\frac{\partial\theta}{\partial Y}\frac{\partial U}{\partial Y} + A_4\,\theta \tag{15}$$

$$\frac{\partial \theta}{\partial t} = B_1 \frac{\partial^2 \theta}{\partial Y^2} + \mathrm{B}_2\, e^{-\beta\theta} \left(\frac{\partial U}{\partial Y}\right)^2 \tag{16}$$

The explicit FDM scheme is given by,

$$U_i^{n+1} = U_i^n + \Delta t A_1 + \Delta t A_2 e^{-\beta\theta_i^n} \frac{U_{i+1}^n - 2U_i^n + U_{i-1}^n}{(\Delta Y)^2} - \Delta t A_3 e^{-\beta\theta_i^n} \left(\frac{\theta_{i+1}^n - \theta_{i-1}^n}{2\Delta Y}\right)\left(\frac{U_{i+1}^n - U_{i-1}^n}{2\Delta Y}\right) + \Delta t A_4 \theta_i^n \tag{17}$$

$$\theta_i^{n+1} = \theta_i^n + \Delta t \left[B_1 \frac{\theta_{i+1}^n - 2\theta_i^n + \theta_{i-1}^n}{(\Delta Y)^2} + B_2 e^{-\beta\theta_i^n} \left(\frac{U_{i+1}^n - U_{i-1}^n}{2\Delta Y}\right)^2\right] \tag{18}$$

Here

$$A_1 = -\frac{\rho_f}{\rho_{hnf}}\frac{\partial \bar{P}}{\partial X}, A_2 = \frac{\rho_f}{\rho_{hnf}}\left(1 + \frac{1}{\lambda}\right)\frac{\mu_{hnf}}{\mu_f}, A_3 = \frac{\rho_f}{\rho_{hnf}}\left(1 + \frac{1}{\lambda}\right)\frac{\mu_{hnf}}{\mu_f}\beta,$$

$$A_4 = Gr, B_1 = \frac{(\rho C_P)_f}{(\rho C_P)_{hnf}}\frac{1}{Pr}\frac{\kappa_{hnf}}{\kappa_f}, B_2 = \frac{(\rho C_P)_f}{(\rho C_P)_{hnf}}\frac{\mu_{hnf}}{\mu_f}Ec$$

Table 2. Comparison of Skin friction(Cf_{avg}) and Nusselt number(Nu_{avg}).

β	Bi	Ec	Cf_{avg}			Nu_{avg}		
			Ali and Makinde [28]	Karim et al. [29]	Current study	Ali and Makinde [28]	Karim et al. [29]	Current study
0.1	1	1.0	0.397	0.395	0.3962	0.512	0.511	0.5121
0.1	3	1.0	0.406	0.405	0.4058	0.790	0.784	0.7883
0.5	1	1.0	0.145	0.146	0.1443	0.223	0.221	0.2227
0.1	1	0.5	0.435	-	0.4347	0.039	-	0.0401
0.1	7	1.0	0.411	-	0.4106	0.943	-	0.9428

4. DISCUSSION OF RESULTS

The governing nonlinear partial differential equations describing the unsteady Casson hybrid nanofluid flow were evaluated numerically using FDM. The impact of various non-dimensional numbers, namely the Casson parameter (λ), Eckert number (Ec), Biot number (Bi), viscosity parameter (β), nanoparticle volume fraction (φ), stretching parameter (γ), and Grashof number (Gr) on velocity, temperature, skin friction, and Nusselt number are presented and interpreted in this section.

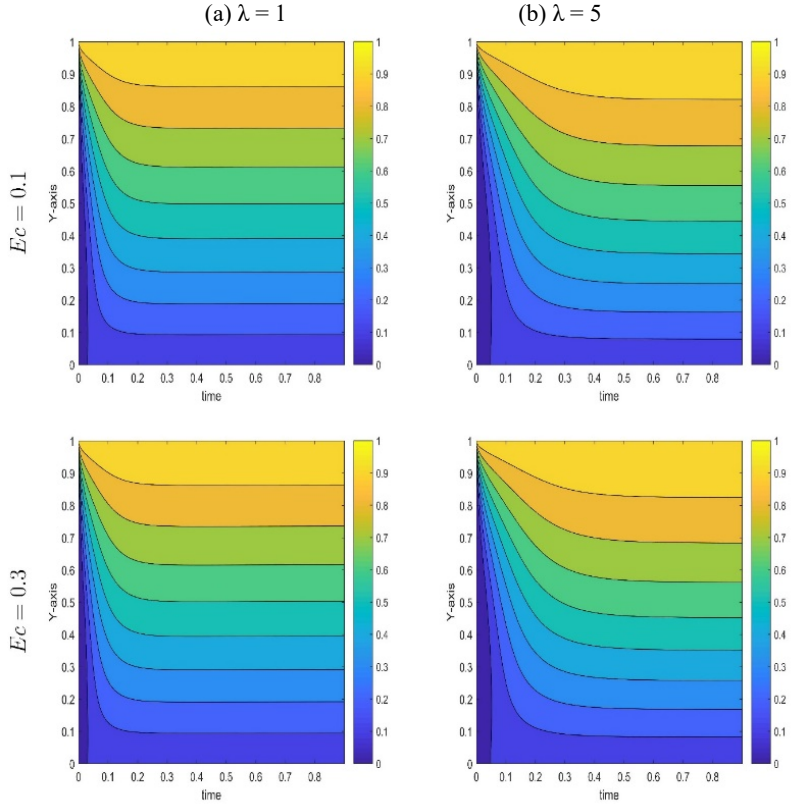

Figure 2. Streamlines for (a) $\lambda = 1$ (b) $\lambda = 5$ and $Ec = 0.1, 0.3$

Figures 2 and 3 illustrate the streamline and isotherm patterns for different values of the Casson parameter λ and Eckert number Ec. It is noticed that with increasing λ (i.e., higher Casson parameter implying stronger yield stress), the flow resistance increases and the velocity gradients near the walls become weaker. Consequently, the flow field becomes more uniform and shear layers are reduced. The isotherm contours reveal that higher λ suppresses heat generation near the moving wall, leading to a more uniform temperature field. An increase in Ec enhances the internal viscous dissipation, which thickens the boundary layer of temperature and raises thermal profile throughout the channel.

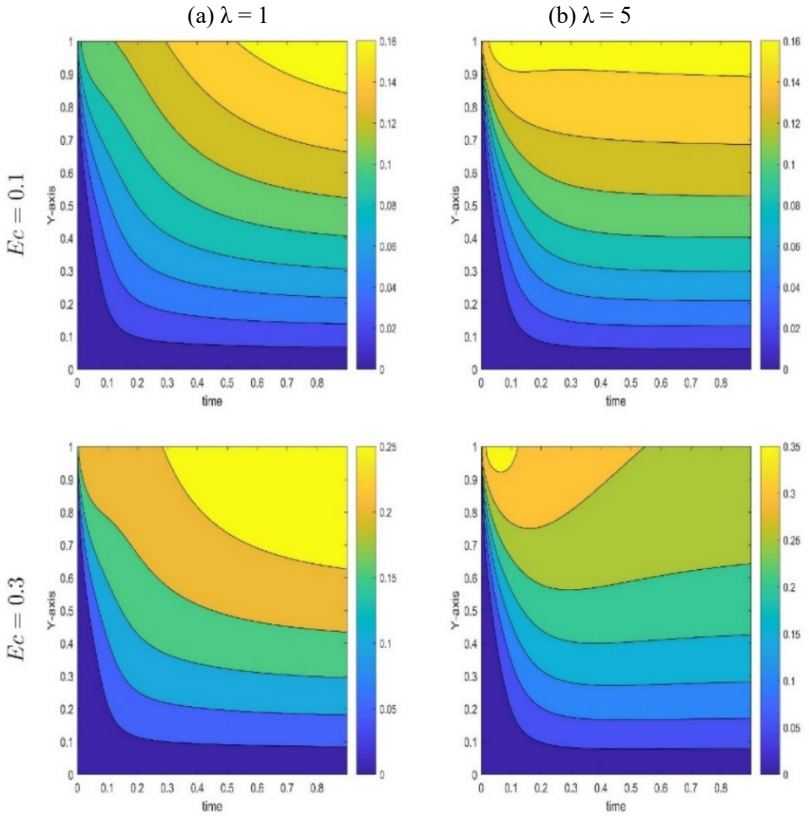

Figure 3. Isotherms for (a) $\lambda = 1$ (b) $\lambda = 5$ and $Ec = 0.1, 0.3$

Figure 4 illustrates that increasing the Biot number decreases slightly the velocity but boosts temperature in the channel. Physically, a larger Bi indicates to enhanced convective heat exchange at the wall. So, there is an increase in wall temperature and consequently the buoyancy-induced motion. As Bi rises, the velocity boundary layer thickens while the temperature gradient near the wall intensifies. This indicates improved heat transfer between the surface and the fluid.

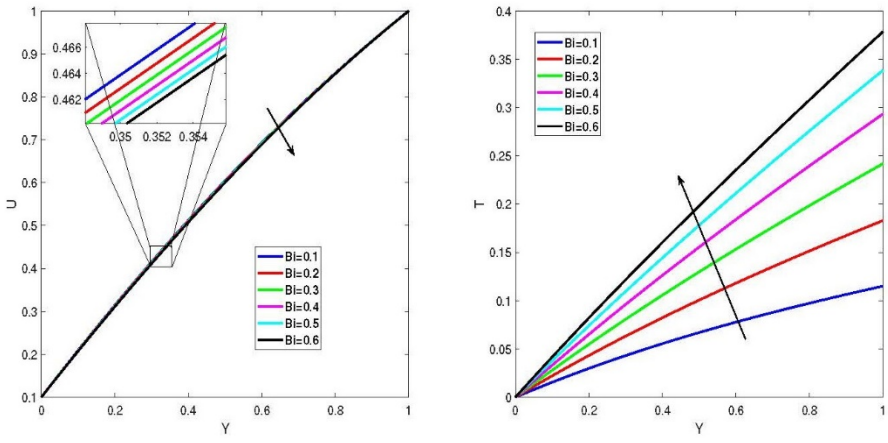

(a) (b)

Figure 4. Effect of Bi on (a) velocity (b) temperature

Eckert number quantifies the conversion of kinetic energy into internal energy due to viscous dissipation. As shown in Figure 5, with higher Ec, the fluid experiences greater frictional heating. This leads to elevated temperature profiles and reduced velocity near the walls. The increase in thermal energy promotes stronger thermal stratification across the channel. This behaviour is consistent with the energy dissipation effects in high-shear flows.

Figure 6 shows that velocity decreases with the increase in β. This is due the increase in effective viscosity, particularly near the lower wall with considerable temperature gradient. Temperature distribution rises with β, as higher viscous resistance dissipates more energy into heat. This trend emphasizes the competing influence between viscous drag and thermal conduction in HNF systems.

Figure 7 shows that increasing the nanoparticle concentration enhances thermal conductivity of the Casson HNF. This leads to higher temperatures throughout the channel. The velocity, however, decreases with increased φ. This is due to the rise in viscosity induced by the additional solid particles. The improved HT demonstrates the synergistic effect of Cu–Al_2O_3 nanoparticles. They provide a better balance between viscosity increase and conductivity improvement compared to single-particle nanofluids.

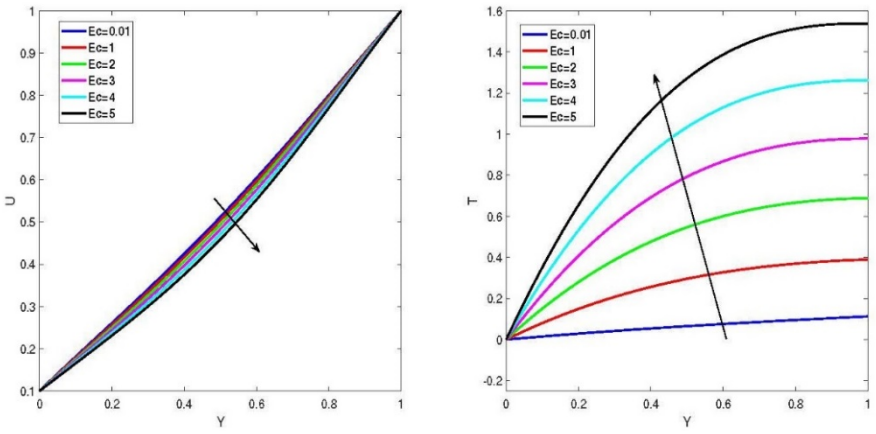

(a) (b)

Figure 5. Effect of Ec on (a) velocity (b) temperature

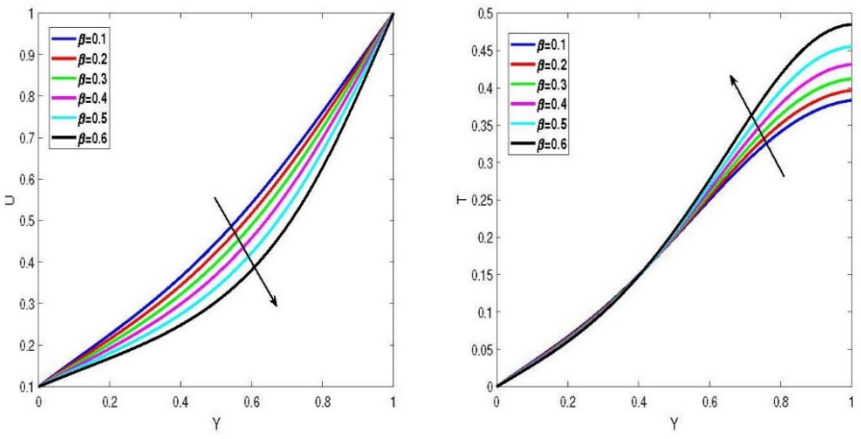

(a) (b)

Figure 6. Effect of β on (a) velocity (b) temperature

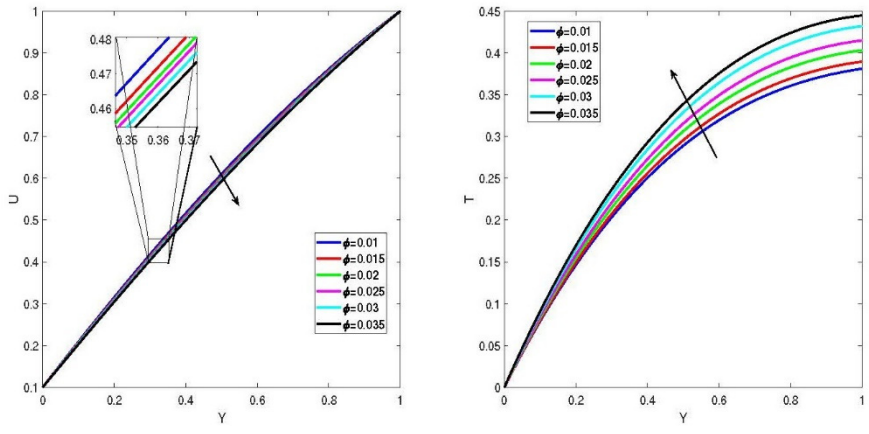

(a) (b)

Figure 7. Effect of ϕ on (a) velocity (b) temperature

From Figure 8, it is evident that increasing γ (the wall stretching rate) accelerates the fluid motion near the lower plate. This leads to higher velocity and thinner velocity boundary layer. The temperature decreases with the increase in γ.

From Figure 9, it is evident that rise in λ values, significantly reduces the fluid velocity and increases temperature. This is due to stronger non-Newtonian effect and higher yield stress. The suppression of motion due to yield stress restricts convective transport, and allows heat to accumulate within the fluid. This behaviour differentiates Casson fluids from Newtonian ones. It also emphasises the significance of rheology concerning HNF performance.

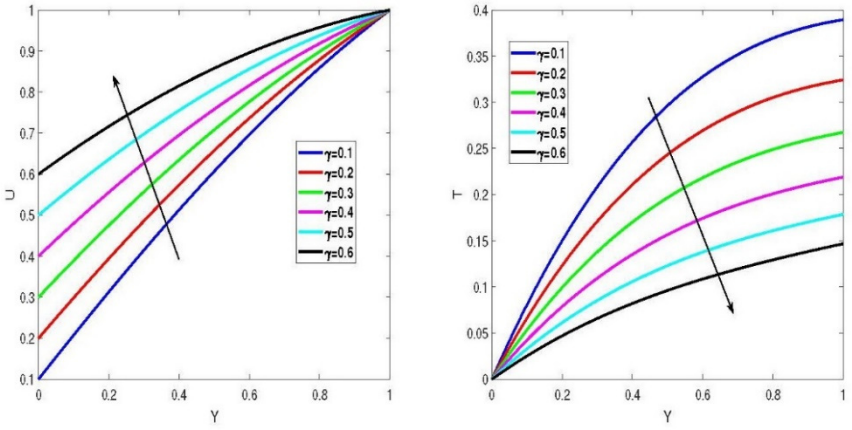

(a) (b)

Figure 8. Effect of γ on (a) velocity (b) temperature

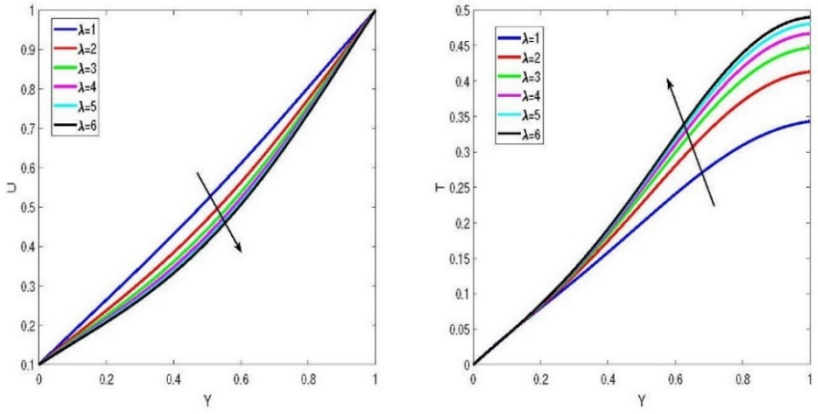

(a) (b)

Figure 9. Effect of λ on (a) velocity (b) temperature

As shown in Figure 10, increasing Gr enhances velocity but decreases temperature field. This happens due to the buoyancy-driven flow formed by temperature gradients. Larger Gr values decrease the temperature slightly. When buoyancy become stronger, the warm fluid is carried away more quickly. This improves cooling effect in the channel of HNF.

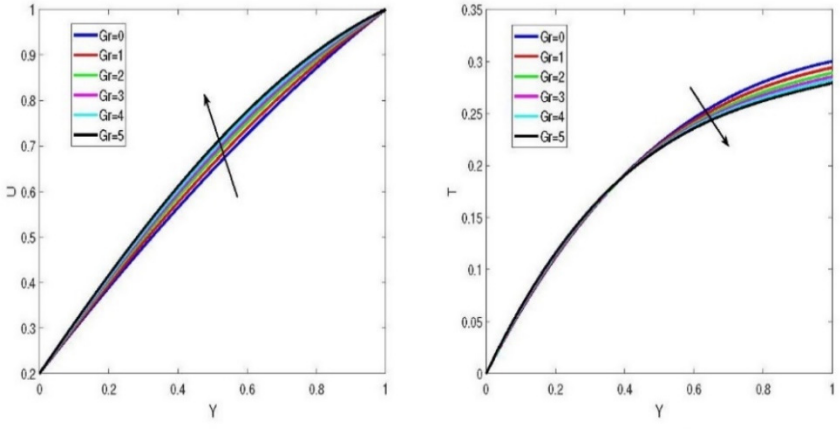

(a) (b)

Figure 10. Effect of Gr on (a) velocity (b) temperature

Figure 11(a) shows that Cf_0 decreases as the Casson parameter increases, while Cf_1 rises. This means that, as the yield-stress increases weaker shear is observed at lower wall but stronger shear at upper wall. Figure 11(b) shows that Nu_0 increases slightly with λ, while the upper wall value Nu_1 decreases. This indicates that higher yield stress enhances HT at the lower plate but reduces it at the upper plate.

Figure 12(a) depicts that, as the Grashof number increases, Cf_0 increases steadily while Cf_1 decreases. Figure 12(b) reveals that Nu_0 increases slightly with Gr, while Nu_1 stays almost same with a tiny downward trend.

Figure 13 reveals that, increasing the Casson parameter λ raises average skin friction but reduces average Nusselt number. Increasing the Grashof number barely affects average friction but slightly boosts average heat transfer.

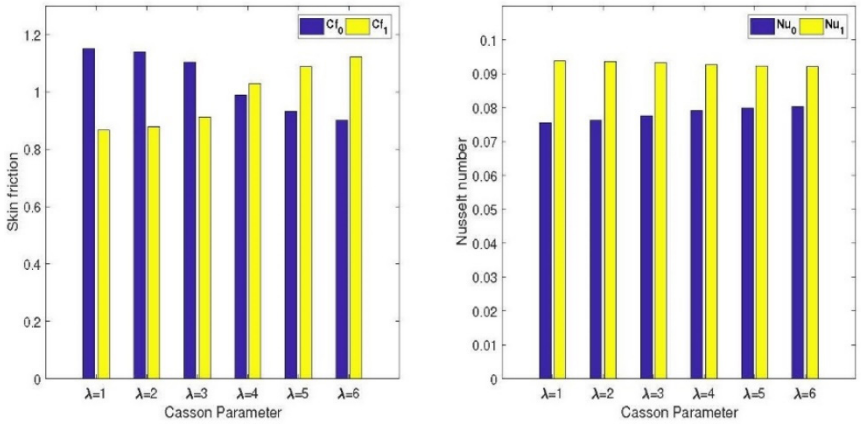

(a) (b)

Figure 11. Effect of λ on (a) Skin friction (b) Nusselt number

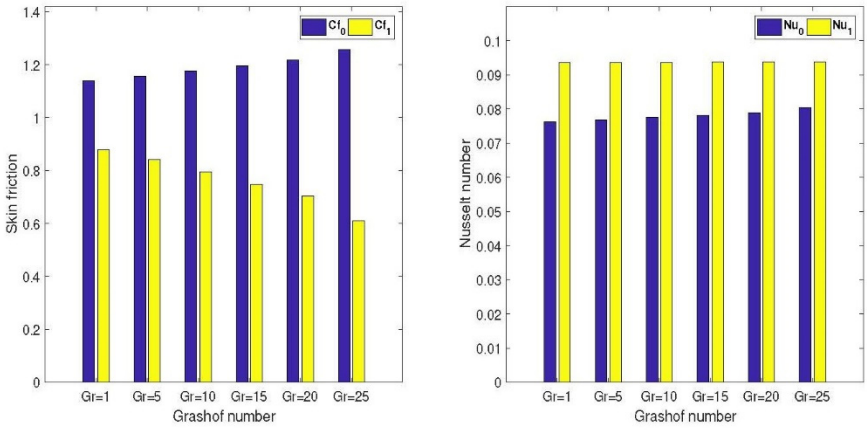

(a) (b)

Figure 12. Effect of Gr on (a) Skin friction (b) Nusselt number

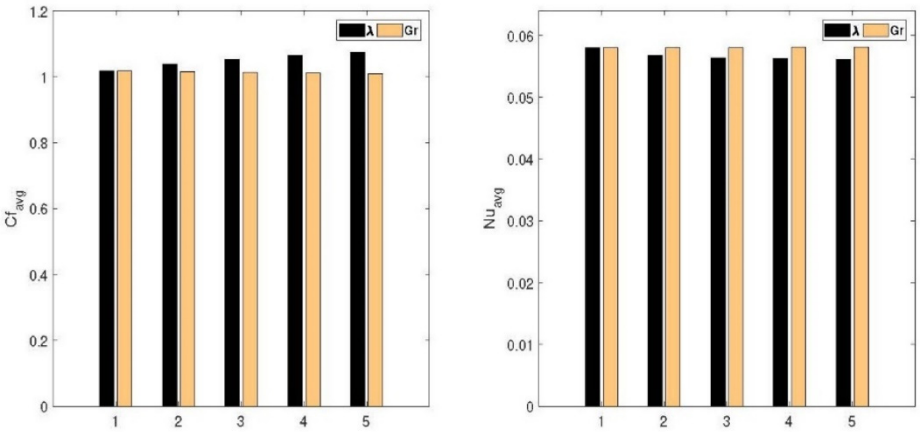

(a) (b)

Figure 13. Variation of average (a) Skin friction (b) Nusselt number for λ and Gr

Figure 14 illustrates the effect of time on the skin friction coefficient (Cf) and Nusselt number (Nu) for $\lambda = 1$ and $\lambda = 2$ over the time interval $t = 0.01 - 1.05$. It is observed that both Cf and Nu exhibit significant variations at early times, indicating transient behaviour. However, as time progresses, the variations gradually diminish, and both quantities approach constant values beyond $t = 1$. Therefore, in the present study, t = 1 is considered as the steady state time. The time step was chosen sufficiently small $dt = 1.3605 \times 10^{-4}$ to ensure convergence of the solution, and further reduction in the time step did not lead to any noticeable change in Cf and Nu.

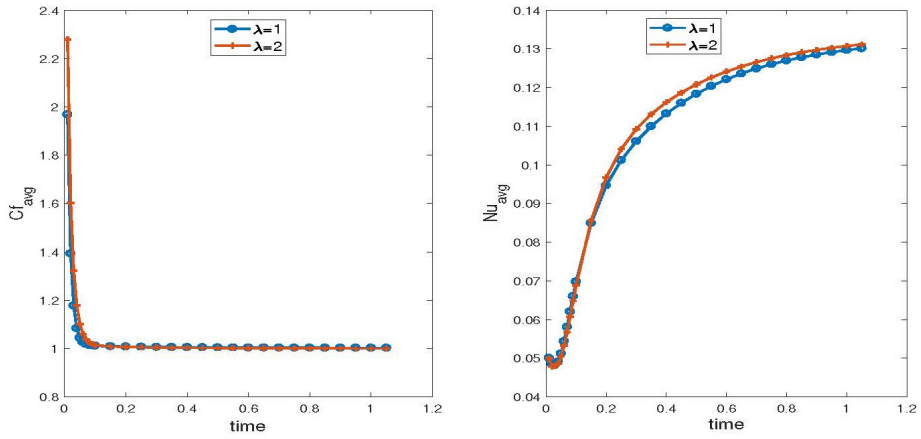

(a) (b)

Figure 14. (a) Skin friction (b) Nusselt number for time variation and $\lambda = 1, 2$

5. CONCLUSIONS

An analysis of unsteady Couette flow and HT behaviour of a Casson HNF composed of copper (Cu) and alumina (Al_2O_3) nanoparticles suspended in water, was carried out through numerical study. Non-dimensional governing equations were evaluated using FDM to study the effects of significant physical parameters for instance, Casson parameter (λ), Grashof number (Gr), Biot number (Bi), Eckert number (Ec), viscosity parameter (β), nanoparticle volume fraction (φ), and wall stretching parameter (γ).

The findings from the study are as follows:

- The momentum field is primarily controlled by rheological and viscous parameters. Casson (λ) and viscosity parameter (β) exert the strongest influence on velocity and skin friction. Higher values of λ significantly suppress fluid motion due to increased yield stress, while larger β enhances viscous resistance. This indicates that non-Newtonian effects dominate momentum transport when λ and β are large.
- The thermal field is mainly governed by the Eckert (Ec) and Biot (Bi) numbers. At low Ec, HT is conduction-dominated, whereas higher Ec leads to dominant viscous dissipation, increased internal heating, thicker thermal layers, and reduced Nusselt numbers. Increasing Bi enhances wall to fluid convection, causing surface convection to dominate thermal transport.
- Buoyancy effects become important at high Grashof numbers (Gr), where natural convection speeds up the flow and improves cooling.
- Nanoparticle volume fraction(ϕ) improve heat transfer by increasing thermal conductivity but reduce fluid velocity because they increase viscosity.
- Stretching parameter(γ) helps control the flow by increasing velocity near wall and reducing fluid temperature, offering useful design control for practical applications.
- From a practical perspective, the results suggest that flow resistance in HNF systems can be effectively controlled through rheological parameters λ and β, whereas thermal performance can be optimized by managing Ec and Bi. These findings provide useful design guidelines for engineering applications such as polymer processing, thermal management systems, and cooling technologies involving non-Newtonian HNFs.

Funding Declaration
The authors declare that no funds, grants, or other financial support were received during the preparation of this manuscript.

ORCID
Khasim Ali, https://orcid.org/0000-0001-8449-7090; **Ramesh Alluguvelli,** https://orcid.org/0000-0002-5075-4375
Chandra Shekar Balla, https://orcid.org/0000-0002-1919-1367

REFERENCES

[1] N. Casson, "A flow equation for the PIGMENT-oil suspensions of the printing ink type," in: *Rheology of Disperse Systems*, edited by C.C. Mill, (Pergamon, 1959), pp. 84–102.

[2] Mukhopadhyay, S., "Casson fluid flow and heat transfer over a nonlinearly stretching surface," Chinese Physics B, **22**(7), 074701 (2013). https://doi.org/10.1088/1674-1056/22/7/074701
[3] M. Abd El-Aziz, and A.A. Afify, "MHD Casson fluid flow over a stretching sheet with entropy generation analysis and Hall influence," Entropy, **21**(6), 592 (2019). https://doi.org/10.3390/e21060592
[4] K. Gangadhar, D.N. Bhargavi, and V.S.R. Munagala, "Steady Boundary Layer Flow of Casson Fluid over a Nonlinear Stretched Sheet in Presence of Viscous Dissipation Using the Spectral Relaxation Method," Mathematical Modelling of Engineering Problems, **7**(3), 351-358 (2020). https://doi.org/10.18280/mmep.070304
[5] I.A. Tantry, S. Wani, and B. Agrawal, "Study of MHD boundary layer flow of a casson fluid due to an exponentially stretching sheet with radiation effect," Int. J. Stat. Appl. Math, **6**, 138-144 (2021). https://doi.org/10.13140/RG.2.2.33054.41286
[6] M.M. Nandeppanavar, "Flow and Heat Transfer Analysis of Casson Fluid due to a stretching sheet: An Analytical Solution," Advances in Physics theories and Applications, **50**, 2224-2225 (2015).
[7] M.B. Ashraf, T. Hayat, and A. Alsaedi, "Mixed convection flow of Casson fluid over a stretching sheet with convective boundary conditions and Hall effect," Boundary Value Problems, **2017**(1), 137 (2017). https://doi.org/10.1186/s13661-017-0869-7
[8] J. Qing, M.M. Bhatti, M.A. Abbas, M.M. Rashidi, and M.E.S. Ali, "Entropy generation on MHD Casson nanofluid flow over a porous stretching/shrinking surface," Entropy, **18**(4), 123 (2016). https://doi.org/10.3390/e18040123
[9] Walawender, W.P., Chen, T.Y. and Cala, D.F., "An approximate Casson fluid model for tube flow of blood," Biorheology, **12**(2), 111-119 (1975). https://doi.org/10.3233/bir-1975-12202
[10] Batra, R.L. and Jena, B., "Flow of a Casson fluid in a slightly curved tube," International journal of engineering science, **29**(10), 1245-1258 (1991). https://doi.org/10.1016/0020-7225(91)90028-2
[11] Pramanik, S., "Casson fluid flow and heat transfer past an exponentially porous stretching surface in presence of thermal radiation," Ain shams engineering journal, **5**(1), 205-212 (2014). https://doi.org/10.1016/j.asej.2013.05.003
[12] Mustafa, M., Hayat, T., Pop, I. and Aziz, A., "Unsteady boundary layer flow of a Casson fluid due to an impulsively started moving flat plate, "Heat Transfer—Asian Research, **40**(6), 563-576 (2011). https://doi.org/10.1002/htj.20358
[13] Shashikumar, N.S., Kumara, B.P., Gireesha, B.J. and Makinde, O.D., "Thermodynamics analysis of MHD Casson fluid slip flow in a porous microchannel with thermal radiation," Diffusion foundations, **16**, 120-139 (2018). https://doi.org/10.4028/www.scientific.net/df.16.120
[14] Choi, S.U.S. "Enhancing thermal conductivity of fluids with nanoparticles," in: *Development and Applications of Non-Newtonian Flows*, edited by D. Singer, and H. Wang, (American Society of Mechanical Engineers, New York, 1995), pp. 99-106.
[15] Tiwari, R.K. and Das, M.K., "Heat transfer augmentation in a two-sided lid-driven differentially heated square cavity utilizing nanofluids," International Journal of heat and Mass transfer, **50**(9-10), 2002-2018 (2007). https://doi.org/10.1016/j.ijheatmasstransfer.2006.09.034
[16] Khan, U., Zaib, A., Pop, I., Waini, I. and Ishak, A., "MHD flow of a nanofluid due to a nonlinear stretching/shrinking sheet with a convective boundary condition: Tiwari–Das nanofluid model," International Journal of Numerical Methods for Heat & Fluid Flow, **32**(10), 3233-3258 (2022). https://doi.org/10.1108/hff-11-2021-0730
[17] Kumar, M., Reddy, G.J., Kumar, N.N. and Bég, O.A., "Computational study of unsteady couple stress magnetic nanofluid flow from a stretching sheet with Ohmic dissipation," Proceedings of the Institution of Mechanical Engineers, Part N: Journal of Nanomaterials, Nanoengineering and Nanosystems, **233**(2-4), 49-63 (2019). https://doi.org/10.1177/2397791419843730
[18] Bao, H.X., Arain, M.B., Shaheen, S., Khan, H.I., Inc, M. and Yao, S.W., "Boundary-layer flow of heat and mass for Tiwari-Das nanofluid model over a flat plate with variable wall temperature," Thermal Science, **26**(Spec. issue 1), 39-47 (2022). https://doi.org/10.2298/tsci22s1039b
[19] Mustafa, M., Khan, J.A., Hayat, T. and Alsaedi, A., "Numerical solutions for radiative heat transfer in ferrofluid flow due to a rotating disk: Tiwari and Das model," International Journal of Nonlinear Sciences and Numerical Simulation, **19**(1), 1-10 (2018). https://doi.org/10.1515/ijnsns-2015-0196
[20] Shekar, B. C., & Kishan, N. "Finite element analysis of natural convective heat transfer in a porous square cavity filled with nanofluids in the presence of thermal radiation," Journal of Physics: Conference Series, **662**(1), 012017 (2015). https://doi.org/10.1088/1742-6596/662/1/012017
[21] Suresh, S., Venkitaraj, K.P., Selvakumar, P. and Chandrasekar, M., "Effect of Al2O3–Cu/water hybrid nanofluid in heat transfer," Experimental Thermal and Fluid Science, **38**, 54-60 (2012). https://doi.org/10.1016/j.expthermflusci.2011.11.007
[22] Waqas, H., Farooq, U., Liu, D., Abid, M., Imran, M. and Muhammad, T., "Heat transfer analysis of hybrid nanofluid flow with thermal radiation through a stretching sheet: A comparative study," International Communications in Heat and Mass Transfer, **138**, 106303 (2022). https://doi.org/10.1016/j.icheatmasstransfer.2022.106303
[23] Muneeshwaran, M., Srinivasan, G., Muthukumar, P. and Wang, C.C., "Role of hybrid-nanofluid in heat transfer enhancement–A review," International Communications in Heat and Mass Transfer, **125**, 105341 (2021). https://doi.org/10.1016/j.icheatmasstransfer.2021.105341; Jha, B. K. "Natural convection in unsteady MHD Couette flow," Heat and mass transfer, **37**(4), 329-331(2001). https://doi.org/10.1007/pl00013295
[24] Rajesh, V. and Öztop, H.F., "Conjugate MHD natural convection in a chamber filled by ternary hybrid nanofluid with entropy generation," Numerical Heat Transfer, Part A: Applications, **86**(19), 6671-6692 (2025). https://doi.org/10.1080/10407782.2024.2344201
[25] Hansda, S., Chattopadhyay, A., Goswami, K.D., Pandit, S.K., Öztop, H.F. and Sheremet, M.A., "Optimizing entropy production in bi-diffusive convection within trapezoidal porous enclosure using radiative trihybrid nanofluids and T-shaped baffle," European Journal of Mechanics-B/Fluids, **113**, 204268 (2025). https://doi.org/10.1016/j.euromechflu.2025.204268
[26] Attia, H. A. "Unsteady hydromagnetic Couette flow of dusty fluid with temperature dependent viscosity and thermal conductivity," International Journal of Non-Linear Mechanics, **43**(8), 707-715 (2008). https://doi.org/10.1016/j.ijnonlinmec.2008.03.007
[27] Ghara, N., Maji, S. L., Das, S., Jana, R., & Ghosh, S. K. "Effects of Hall current and ion-slip on unsteady MHD Couette flow," Open Journal of Fluid Dynamics, **2**(01), 1 (2012). https://doi.org/10.4236/ojfd.2012.21001
[28] K. Jha, B., & A. Apere, C. "Combined effect of hall and ion-slip currents on unsteady mhd couette flows in a rotating system," Journal of the Physical Society of Japan, **79**(10), 104401 (2010). https://doi.org/10.1143/jpsj.79.104401
[29] Guria M, Jana RN, Ghosh SK, "Unsteady Couette flow in a rotating system," Int. J. Non-Linear Mech. **41**, 838–843 (2006). https://doi.org/10.1016/j.ijnonlinmec.2006.04.010

[30] Ali, A. O., & Makinde, O. D. "Modelling the Effect of Variable Viscosity on Unsteady Couette Flow of Nanofluids with Convective Cooling," Journal of Applied Fluid Mechanics, **8**(4), 793-802 (2015). https://doi.org/10.18869/acadpub.jafm.67.223.22967
[31] Karim, M. E., Samad, M. A., & Ferdows, M. "Numerical study of the effect of variable viscosity on unsteady pulsatile nanofluid flow through a Couette channel of stretching wall with convective heat transfer," AIP Conference Proceedings, **2121**(1), 070005 (2019). https://doi.org/10.1063/1.5115912
[32] Hajmohammadi, M. R. "Cylindrical Couette flow and heat transfer properties of nanofluids; single-phase and two-phase analyses," Journal of Molecular Liquids, **240**, 45-55 (2017). https://doi.org/10.1016/j.molliq.2017.05.043
[33] Wakif, A., Boulahia, Z., Ali, F., Eid, M. R., & Sehaqui, R. "Numerical analysis of the unsteady natural convection MHD Couette-nanofluid flow in the presence of thermal radiation using single and two-phase nanofluid models for Cu-water nanofluids," International Journal of Applied and Computational Mathematics, **4**(3), 1-27 (2018). https://doi.org/10.1007/s40819-018-0513-y
[34] Zeeshan, A., Khan, M.I., Ellahi, R. and Marin, M., "Computational intelligence approach for optimising MHD Casson ternary hybrid nanofluid over the shrinking sheet with the effects of radiation," Applied Sciences, **13**(17), 9510 (2023). https://doi.org/10.3390/app13179510
[35] Akbar, N.S., Hussain, M.F., Alghamdi, M. and Muhammad, T., "Thermal characteristics of magnetized hybrid Casson nanofluid flow in a converging–diverging channel with radiative heat transfer: A computational analysis," Scientific Reports, **13**(1), 21891 (2023). https://doi.org/10.1038/s41598-023-49397-3
[36] Das, S., Ali, A. and Jana, R.N., "Insight into the dynamics of magneto-casson hybrid nanoliquid caused by a plate rotation," World Journal of Engineering, **18**(1), 66-84 (2021). https://doi.org/10.1108/wje-07-2020-0261
[37] Krishna, M.V., "Hall and ion slip effects on the MHD flow of Casson hybrid nanofluid past an infinite exponentially accelerated vertical porous surface," Waves in Random and Complex Media, **34**(5), 4658-4687 (2024). https://doi.org/10.1080/17455030.2021.1998727
[38] Mishra, S.R., Mathur, P. and Pattnaik, P.K., "Hybrid nanofluid flow of non-Newtonian Casson fluid for the analysis of Entropy through a permeable medium," Journal of Nanofluids, **11**(3), 328-339 (2022). https://doi.org/10.1166/jon.2022.1846
[39] Rehman, A., Khan, D., Mahariq, I., Elkotb, M.A., and Elnaqeeb, T., "Viscous dissipation effects on time-dependent MHD Casson nanofluid over stretching surface: A hybrid nanofluid study," Journal of Molecular Liquids, **408**, 125370 (2024). https://doi.org/10.1016/j.molliq.2024.125370
[40] Varatharaj, K., Tamizharasi, R., Sivaraj, R. and Vajravelu, K., "Simulation of MHD-Casson hybrid nanofluid dynamics over a permeable stretching sheet: effects of heat transfer and thermal radiation," Journal of Thermal Analysis and Calorimetry, **149**(15), 8693-8711 (2024). https://doi.org/10.1007/s10973-024-13347-6
[41] Balla, C.S., Ali, K. and Rajashekhar Reddy, Y., "Effectiveness of silver-magnesium oxide-water hybrid nanofluid in Couette channel," Proceedings of the Institution of Mechanical Engineers, Part N: Journal of Nanomaterials, Nanoengineering and Nanosystems, **239**(1-2), 3-10 (2025). https://doi.org/10.1177/23977914231196379
[42] Ali, K., Reddy, Y.R. and Shekar, B.C., "Thermo-fluidic transport process in magnetohydrodynamic Couette channel containing hybrid nanofluid," Partial Differential Equations in Applied Mathematics, **7**, 100468 (2023). https://doi.org/10.1016/j.padiff.2022.100468
[43] Raza, A., Almusawa, M.Y., Ali, Q., Haq, A.U., Al-Khaled, K. and Sarris, I.E., "Solution of water and sodium alginate-based casson type hybrid nanofluid with slip and sinusoidal heat conditions: A prabhakar fractional derivative approach," Symmetry, **14**(12), 2658 (2022). https://doi.org/10.3390/sym14122658
[44] Paul, A., Sarma, N. and Patgiri, B., "MHD Al2O3/Cu-water Casson hybrid nanofluid flow across a porous exponentially stretching sheet," Latin American Applied Research-An international journal, **54**(4), 467-476 (2024). https://doi.org/10.52292/j.laar.2024.3282
[45] Reddy, V.S., Kandasamy, J. and Sivanandam, S., "Impacts of casson model on hybrid nanofluid flow over a moving thin needle with dufour and soret and thermal radiation effects," Mathematical and Computational Applications, **28**(1), 2 (2022).
[46] Sarkar, A., Mondal, H. and Nandkeolyar, R., "Mixed convective hydromagnetic unsteady Casson hybrid nanofluid flow analysis and entropy optimization over an inclined surface with viscous dissipation," Discover Molecules, **2**(1), 10 (2025).
[47] Ishaq, M., Khan, S.U., Garalleh, H.A., Sowayan, A.S. and Tlili, I., "Thermal performance of casson hybrid nanofluid with radiative effects and convective conditions: applications to energy systems and industrial heat transfer," Multiscale and Multidisciplinary Modeling, Experiments and Design, **8**(2), 141 (2025). https://doi.org/10.1007/s41939-024-00720-z

FDM-МОДЕЛЮВАННЯ ПОТОКУ ТА ТЕПЛОПЕРЕНОСУ ГІБРИДНОЇ НАНОРІДИНИ КАССОНА Cu–Al_2O_3/ВОДА В СИСТЕМІ КУЕТТА

Хасім Алі[1], Рамеш Аллугувеллі[2], Сватмарам[3], Чандра Шекар Балла[4], К. Правін Кумар[5], Е. Джагатпрабхав[6]
[1]Кафедра математики, інженерно-технологічний коледж імені Наваба Шаха Алама Хана, Хайдерабад, Телангана, 500024, Індія
[2]Кафедра математики, інженерно-технологічний коледж імені Гітанджалі, Кісара, Хайдерабад, Телангана, 501303, Індія
[3]Кафедра математики, технологічний інститут Чайтаньї Бхаратхі, Хайдерабад, Телангана, 500075, Індія
[4]Урядовий молодший коледж, Амангал, Ранга Редді, Телангана, 509321, Індія
[5]Кафедра гуманітарних наук та природничих наук, державний політехнічний інститут, Хайдарабад, Телангана, 500028, Індія
[6]Кафедра гуманітарних наук та природничих наук, державний політехнічний інститут, Шаднагар, Телангана, 509216, Індія

У цій статті чисельно досліджується нестаціонарна гібридна нанорідина Куетта-Кассона (HNF), що містить наночастинки міді (Cu) та оксиду алюмінію (Al_2O_3), розчинені у воді. Верхня стінка приводиться в рівномірний рух, а нижня стінка вважається нерухомою та розтяжною. Для інтегрування керованих нелінійних диференціальних рівнянь з частинними похідними використовується метод скінченних різниць (FDM). Результати досліджуються за допомогою ліній струму, ізотерм, числа Нуссельта та поверхневого тертя. Обговорюється вплив ключових безрозмірних чисел, таких як число Грасгофа, число Біо, параметр розтягування, параметр Кассона та число Екерта, на HNF Cu-Al_2O_3-вода. Результати показують, що потік та теплопередача (HT) можуть значною мірою контролюватися ключовими параметрами.

Ключові слова: *потік Куетта; змінна в'язкість; нанорідина Al_2O_3-H_2O; число Біо; параметр розтягування*